Acta Biomaterialia 95 (2019) 319–327

Contents lists available at ScienceDirect

Acta Biomaterialia

journal homepage: www.elsevier.com/locate/actabiomat

Full length article

3D printed micro-scale force gauge arrays to improve human cardiac tissue maturation and enable high throughput drug testing ☆

Xuanyi Ma [a], Sukriti Dewan [a], Justin Liu [b], Min Tang [c], Kathleen L. Miller [c], Claire Yu [c], Natalie Lawrence [c], Andrew D. McCulloch [a,d], Shaochen Chen [a,b,c,e,*]

[a] Department of Bioengineering, University of California San Diego, 9500 Gilman Drive, La Jolla, CA 92093, USA
[b] Department of Materials Science and Engineering Program, University of California San Diego, 9500 Gilman Drive, La Jolla, CA 92093, USA
[c] Department of NanoEngineering, University of California San Diego, 9500 Gilman Drive, La Jolla, CA 92093, USA
[d] Department of Medicine, University of California San Diego, 9500 Gilman Drive, La Jolla, CA 92093, USA
[e] Chemical Engineering Program, University of California San Diego, 9500 Gilman Drive, La Jolla, CA 92093, USA

ARTICLE INFO

Article history:
Received 4 September 2018
Received in revised form 11 December 2018
Accepted 17 December 2018
Available online 19 December 2018

Keywords:
3D printing
iPSC-derived cardiomyocytes
Cardiac force measurement
Drug testing

ABSTRACT

Human induced pluripotent stem cell – derived cardiomyocytes (iPSC-CMs) are regarded as a promising cell source for establishing *in-vitro* personalized cardiac tissue models and developing therapeutics. However, analyzing cardiac force and drug response using mature human iPSC-CMs in a high-throughput format still remains a great challenge. Here we describe a rapid light-based 3D printing system for fabricating micro-scale force gauge arrays suitable for 24-well and 96-well plates that enable scalable tissue formation and measurement of cardiac force generation in human iPSC-CMs. We demonstrate consistent tissue band formation around the force gauge pillars with aligned sarcomeres. Among the different maturation treatment protocols we explored, 3D aligned cultures on force gauge arrays with in-culture pacing produced the highest expression of mature cardiac marker genes. We further demonstrated the utility of these micro-tissues to develop significantly increased contractile forces in response to treatment with isoproterenol, levosimendan, and omecamtiv mecarbil. Overall, this new 3D printing system allows for high flexibility in force gauge design and can be optimized to achieve miniaturization and promote cardiac tissue maturation with great potential for high-throughput *in-vitro* drug screening applications.

Statement of Significance

The application of iPSC-derived cardiac tissues in translatable drug screening is currently limited by the challenges in forming mature cardiac tissue and analyzing cardiac forces in a high-throughput format. We demonstrate the use of a rapid light-based 3D printing system to build a micro-scale force gauge array that enables scalable cardiac tissue formation from iPSC-CMs and measurement of contractile force development. With the capability to provide great flexibility over force gauge design as well as optimization to achieve miniaturization, our 3D printing system serves as a promising tool to build cardiac tissues for high-throughput *in-vitro* drug screening applications.

1. Introduction

Cardiovascular disease remains a major cause of morbidity and mortality worldwide [1]. For this reason, drug discovery and mechanistic investigation of cardiovascular diseases have been critical research areas of focus [2,3]. Human induced pluripotent stem cell-derived cardiomyocytes (iPSC-CMs), with potential to represent individual variations, are candidates for translatable drug screening and personalized medicine [4,5]. However, the drug screening and disease modeling applications of these derived cells have been limited by their immature phenotypes and limited capacity for physiological force development [6,7].

Approaches to promoting mature cardiomyocyte phenotypes, such as the use of 3D aligned cultures [8,9], mechanical stretching [9–11], and electrical pacing [9,11,12] have been shown to improve

☆ Part of the Cell and Tissue Biofabrication Special Issue, edited by Professors Guohao Dai and Kaiming Ye.

* Corresponding author at: Department of NanoEngineering, University of California San Diego, 9500 Gilman Drive, Mail code 0448, La Jolla, CA 92093-0448, USA.
E-mail address: chen168@eng.ucsd.edu (S. Chen).

https://doi.org/10.1016/j.actbio.2018.12.026
1742-7061/

functional performance. In particular, these techniques have been applied to various engineered heart tissue (EHT) systems to maturate *in-vitro* human cardiac tissues. For example, mechanical stimulation was applied to human embryonic stem cell (ESC)-derived cardiomyocytes in 3D collagen matrix and electrical pacing was used to induce synchronized beating in an iPSC-derived 3D cardiac tissue [10,13]. Nevertheless, none of the current human platforms demonstrated cardiac tissue force measurements directly following tissue maturation in a high-throughput format. Without the potential to scale up tissue maturation and force measurements, the application of iPSC-derived cardiac tissues in translatable drug screening remains limited. Therefore, there is a critical need to combine maturation approaches with high-throughput force gauge platform to study cardiac tissue drug response in a scalable format.

Traditional microfabrication technologies, such as those based on polyacrylamide and polydimethylsiloxane (PDMS), have been used to fabricate miniaturized structures with scalable potential [14,15]. However, these approaches mostly take multiple steps to complete and are limited in flexibility of design adjustment. Micro-scale continuous optical printing (μCOP), which is a type of digital light processing (DLP)-based 3D printing, provides a superior speed and scalability for the fabrication of micro-scale complex 3D constructs [16–20]. In addition, the use of digital pattern designs offers great flexibility to fabricate and optimize 3D printed structures [16–20]. In this report, we present a micro-scale force gauge platform based on micro-pillars fabricated by μCOP for cardiac tissue maturation, force measurement, and studying drug response. This printed array of micro-scale force gauges was customized to fit into a regular 24-well and 96-well plate for seeding of iPSC-CMs to form micro-tissues for high-throughput studies. Upon testing different protocols of tissue maturation treatment, 3D aligned culture on force gauge with in-culture pacing showed the highest expression of maturation cardiac genes when compared to the three other culture methods. Moreover, micro-tissues cultured using the optimized pillar design and maturation method generated the largest force with increased force outputs following incubation with drugs such as isoproterenol (ISO), levosimendan (LEVO) and omecamtiv mecarbil (OM). Overall, we have demonstrated that our 3D printing system is a promising tool to fabricate *in-vitro* cardiac tissues that are functionally mature for drug screening in a high-throughput format.

2. Materials and methods

2.1. Photoinitiator synthesis

Photoinitiator lithium phenyl-2,4,6 trimethylbenzoylphosphinate (LAP) was synthesized as previously reported [17,19]. In brief, a total of 3.2 g (0.018 mol) of 2,4,6-trimethylbenzoyl chloride (Acros Organics) was added drop by drop to an equimolar amount of dimethyl phenylphosphonite (3.0 g; Sigma-Aldrich) with continuously stirring. The reaction mixture was then stirred for 18 h at room temperature and under argon. The mixture was then heated to 50 °C. A four-fold excess of lithium bromide (6.1 g; Sigma Aldrich) in 100 mL of 2-butanone (Sigma-Aldrich) was added. After 10 min, a solid precipitate was formed. The mixture was cooled to room temperature, and allowed to rest for 4 h. The filtrate was washed and filtered 3 times with 2-butanone to remove unreacted lithium bromide. Excess solvent was removed by vacuum. Dried powders of LAP was then stored in dark at −20 °C.

2.2. Pre-polymer preparation

Poly (ethylene glycol) diacrylate (PEGDA, MW 700), 2-hydroxy-4-methoxy-benzophenon-5-sulfonic acid (HMBS), and 4-hydroxy-TEMPO (TEMPO) were purchased from Sigma-Aldrich. Free radical quencher TEMPO and UV absorber HMBS were first dissolved in ethanol and water to make a 2% and a 1% stock solution, respectively. Photoinitiator LAP synthesized as described above was dissolved in water to make a 3% stock solution. The final prepolymer solution was composed of 40% PEGDA, 0.2% (wt/vol) LAP, 0.002% (wt/vol) TEMPO, and 0.2% (wt/vol) HMBS. The solution was sonicated for 1 h to ensure complete mixing.

2.3. 3D printing of micro-pillar construct

To build a high throughput miniaturized platform that can fit into a regular 96-well setup, a pattern consisting of an array of eight pillar set was designed. DLP-based 3D printing was chosen as the fabrication method for its superior fabrication speed, scalability and flexibility in fabricating micro-scale complex 3D constructs [16–20]. The patterns of the micro-pillar array were designed in Adobe Photoshop with dimensions compatible to a digital micromirror device (DMD). Each pattern was assigned a UV exposure duration. The micro-pillar construct was fabricated using the μCOP 3D printing system, by simultaneously moving the stage in the Z direction and projecting the patterns through DMD on the printing compartment with the prepolymer solution. To prepare the printing compartment, 500 μm-thick PDMS spacers were placed on a glass slide to control the structure height. A methacrylated glass coverslip was placed on top of the spacers. The pre-polymer solution was stored in dark at 4 °C and injected into the compartment immediately before printing. The structure was printed within 30 s, and then washed with PBS and sterilized with UV light for 1 h. Sterile constructs were stored in PBS at 4 °C before use. The entire printed array is 2.7 × 3 mm, with a height of 500 μm. The cross-section dimension for the thin pillar is 60 × 135 μm and for the thick pillar is 135 × 135 μm. The distance between the thin and thick pillars were set to 175, 200 and 225 μm depending on the experimental conditions.

2.4. Mechanical testing

After 3D printing, the thick and thin pillars without seeded cells were tested for their mechanical properties at 24 h, 72 h, 7 day and 14 day time points in PBS at 37 °C and 5% CO_2. There are 5 samples for each time point. Pillars with seeded cells were also tested for their mechanical properties. Particularly, iPSC-CMs at a final density of 7.5 millions/mL were seeded into microwells. The thin pillar, i.e. the bending pillar, were tested at 24 h and 7 day time points following cell seeding, with the 7 day time point also being the force measurement time point. There were 5 samples for 24 h time point and 12 samples for 7 day time point. Before each time point of measurement, samples with seeded cells were incubated at 37 °C and 5% CO_2 following printing. Mechanical property measurement of the pillars was carried out using a commercial MicroSquisher (CellScale). The measurement and analysis focused only on the elastic modulus of the pillar. Bending tests were carried out by using metal beams to bend the pillar at the height of the micro-tissue to achieve 10% displacement. The elastic modulus was calculated from the force and displacement data collected by MicroSquisher. Customized MATLAB scripts were used for data analysis and modulus calculation.

2.5. Neonatal cardiomyocyte isolation and culture

NVCM were isolated from the hearts of neonates of CD-1 wild-type mice (Charles River Labs). All animal procedures followed the Guide for the Care and Use of Laboratory Animals (8th ed.) and were approved by the University of California San Diego Institutional Animal Care and Use Committee (IACUC) (protocol

no. S01013M). In brief, hearts were surgically removed from 1-day-old to 2-day-old pups and digested in Hank's Balanced Salt Solution (Gibco) with 0.046% (wt/vol) Trypsin (Affymetrix) at 4 °C overnight. Blood cells were removed from hearts by type II Collagenase (Worthington) after shaking at 37 °C for 2 min. A heterogenous cell population containing cardiomyocytes and fibroblasts was isolated after further digestion using type II Collagenase (Worthington) at 37 °C for 7 min. Fibroblasts were removed by pre-plating for 1.5 h on 75 cm^2 plastic tissue culture flasks (Corning) in a humidified incubator at 37 °C with 5% CO_2. Isolated cardiomyocytes were resuspended at 12 millions/mL in dark medium formulated by 75% (vol/vol) DMEM and 25% (vol/vol) M199 medium containing 10 mM HEPES, 10% (vol/vol) horse serum (hyclone) and 5% (vol/vol) fetal bovine serum (Gibco), 1% (vol/vol) 100x Penicilin/Streptomycin/L-Glutamine solution (Gibco).

2.6. Integration-free human iPSCs generation

Human iPSCs were re-programmed as previously described [16,17]. In brief, human adult dermal fibroblasts (HDF, Cell Applications) and human perinatal foreskin fibroblasts (BJ, ATCC) were maintained in DMEM (Corning) supplemented with Antibiotics/Antimicotic (Corning) and 10% (vol/vol) Fetal Bovine Serum (Tissue Culture Biologicals) in a 37 °C, 5% CO_2 incubator. Both types of cells were passaged by 0.25% Trypsin-EDTA (Corning) every 3–5 days at a ratio of 1:6 before reprogramming. In preparation for reprogramming, fibroblasts were seeded in 6-well plates at a density of 2×10^5 cells per well. They were allowed to attach and spread for 48 h. Reprogramming was performed by using a Sendai virus-based Cyto Tune kit (Life technologies) following manufacturer's instructions for the delivery of four factors Oct4, Sox2, Klf4 and c-Myc. Successful clones were later picked and maintained in Essential 8 medium.

2.7. Human iPSC culture and cardiac differentiation

Following successful reprogramming, hESC-qualified matrigel (Corning) was used as the substrate matrix for the maintenance of human iPSCs culture in xeno- and feeder-free Essential 8 medium (Life Technologies) following the manufacturer's instructions. Cells were split at a ratio of 1:8 every 3–4 days by Versene (Life Technologies) before experiments. To prepare for differentiation, iPSCs were digested by Versene (Life Technologies) and seeded in matrigel coated 12-well plates at 1:8 ratio. Seeded cells were maintained in Essential 8 medium before reaching 80% confluency.

Cardiac differentiation (Supplementary Fig. 3) was initiated using the PSC Cardiomyocytes Differentiation Kit (Cat. # A25042SA, Life Technologies). Human iPSCs were first cultured in medium A for 48 h and subsequently cultured in cardiomyocyte differentiation medium B for another 48 h. After the initial 4 days, the cells were cultured in cardiomyocyte maintenance medium for 8 more days. Spontaneous beating was observed on day 8–9 of differentiation. On day 12, differentiated cells were purified by incubating in RPMI1640 medium without glucose (Life Technologies) supplemented with 4 mM lactate (Wako Pure Chemical) for an additional 6–7 days [21]. Purified cardiomyocytes were then cultured in HEPES buffered RPMI1640 medium (Life Technologies) supplemented with 2% (vol/vol) B27 (Life Technologies) until the day for pillar seeding. To prepare the cells for seeding into 3D printed structure, iPSC-CMs were dissociated with 0.25% trypsin-EDTA for 5–7 min, pelleted at 200 g for 3 min with the supernatant removed. Cells were resuspended in resuspension medium composed of RPMI1640 medium (Life Technologies) with 20% (vol/vol) FBS (Gibco) and 5 μM ROCK Inhibitor Y-27632 (STEMCELL Technologies) at a concentration of 15 millions/mL. Cell suspension was placed on ice and used immediately.

2.8. Cyclic stretching of iPSC-CM

Flexcell(R) Tissue Train(R) Culture System was set up in a regular incubator according to manufacturer's instructions. Commercially available laminin coated UniFlex® culture plates (Flexcell) with PDMS membrane bottom were prepared. Human iPSC-CMs, following purification by lactate conditioned medium, were seeded in 6-well UniFlex® culture plates according to manufacture's instructions. When iPSC-CMs formed a confluent monolayer culture, unidirectional stretch, set at 5% elongation, was carried out for 7 days at 0.5 Hz. Following the stretching period, cells were cultured in regular static condition until their detachment and seeding in printed constructs.

2.9. Scaffold seeding and maintenance

Before cell seeding, the fabricated micro-pillar structures were stored in PBS with 1% (vol/vol) 100x Penicilin/Streptomycin/L-Glu tamine solution (Gibco) followed by 1 h UV irradiation. To prepare for seeding, the printed constructs were placed in a sterile well plate and let air dried in biosafety cabinet. Pre-cooled material mixture, consisting of 3 mg/mL liquid pH neutralized rat tail collagen I (Corning) and 1 mg/mL bovine plasma fibrinogen (Sigma-Aldrich), was mixed at 1:1 vol ratio with freshly isolated neonatal cardiomyocyte suspension. Similarly for human iPSC-CM, pre-cooled material mixture, consisting of 2 mg/mL liquid pH neutralized rat tail collagen I (Corning) and 1 mg/mL bovine plasma fibrinogen (Sigma-Aldrich), was mixed at 1:1 vol ratio with human iPSC-CM suspension. The cell-material mixture solution was then added to the top surface of the constructs to form a droplet. The well plates were then centrifuged at 200 g for 1 min to load cell-material mixture into the micro-wells with micro-pillars. Excess cell-gel mixture was removed by aspirating the surrounding of the construct before incubating in a humidified incubator at 37 °C with 5% CO_2 for 30 min to induce collagen polymerization. Following the 30 min incubation, warm dark medium (for NVCM) or iPSC-CM resuspension medium (for iPSC-CM) was then added to construct wells in culture plates. Samples were incubated overnight in a humidified incubator at 37 °C with 5% CO_2, and additional medium was added the following day. After that, medium change was performed every day until the measurement day. For iPSC-CM samples, resuspension medium was switched to RPMI1640 medium (Life Technologies) supplemented with 2% (vol/vol) B27 (Life Technologies) on day 2 following seeding. For in-culture paced conditions, customized platinum electrodes that attached to the plate lid were made to fit in commercially available well plates. Cardiac tissues on force gauges were paced at 0.3 Hz every other day starting day 4 following cell seeding. In particular, we implemented several approaches to prevent cell death from pacing and did not notice a significant increase in dead cells after our pacing protocol. Specifically, we added ascorbic acid in culture medium for all our conditions as ascorbic acid has shown to reduce the generation of reactive oxygen species and alleviate stress-induced damage in cardiomyocytes [22,23]. Secondly, we paced on alternative days and only for for two full days in total, and replaced fresh medium immediately following pacing to prevent cell death from prolonged pacing or used medium.

2.10. Immunofluorescent staining and imaging

Samples were fixed in 4% (wt/vol) paraformaldehyde solution (Wako) for 15 min at room temperature on day 3 (for NVCM) and day 7 (for iPSC-CM) following seeding respectively. They were subsequently blocked and permeabilized with 2% (wt/vol) bovine serum albumin (BSA) (Gemini Bio-Products) solution with 0.1% (vol/vol) Triton X-100 (Promega) for 1 h at room temperature.

Samples were then incubated with mouse monoclonal antibodies against alpha-actinin (1:100, Sigma) and rabbit monoclonal antibodies against connexin 43 (1:100, Cell Signaling Technology) overnight at 4 °C. Following primary antibody incubation, samples were washed three times with PBS at room temperature, followed by 1 h room temperature incubation with fluorophore-conjugated anti-IgG antibodies (1:200, Biotium). Hoescht 33258 (Invitrogen) nucleus counterstain was also performed. Following 3 times of washing with PBS (Gibco, Life Technologies), fluorescently stained samples were stored in PBS (Gibco, Life Technologies) with 0.05% (wt/vol) sodium azide (Alfa Aesar) at 4 °C and imaged within 1 week of staining.

2.11. RNA isolation and reverse transcription-polymerase chain reaction (RT-PCR)

Samples were treated with ice cold TRIzol reagent (Ambion, Life Technologies) and pipetted for 5 min before storage in −80 °C fridge for RNA extraction. To ensure enough RNA was collected, 4–8 tissue constructs under the same condition were pooled together. Total RNA from each TRIzol sample was isolated using Direct-zol RNA MiniPrep Kit (Zymo Research) according to the manufacturer's instruction. Extracted RNA samples were stored in −80 °C freezer before RT-PCR experiments.

Reverse transcription was carried out to synthesize cDNA using PhotoScript® first strand cDNA synthesis kit (New England BioLabs) according to manufacturer's instruction. Real-time RT-PCR was performed using KAPA SYBR Fast qPCR kit (KAPA Biosystems) with specific primers (Integrated DNA Technologies) and detected by StepOne™ Real-Time PCR System (ThermoFisher). Relative quantification was carried out based on the threshold cycle (Ct) of each sample and the values were normalized against the housekeeping gene, glyceraldehyde 3-phosphate dehydrogenase (GAPDH).

2.12. Drug incubation

Three drugs, ISO (100 nM), LEVO (1 μM), and OM (200 nM) were used to study their corresponding effects on the iPSC-derived cardiac tissue on day 7 following seeding onto the pillar. Specifically, samples were firstly incubated in Tyrode's solution (containing 1.4 mM calcium ions). The displacement traces of the thin pillar due to cardiac tissue contraction without any drug treatment were recorded as untreated paired controls. Following the initial recording, samples were treated with each one of the three drugs at the specified concentration in Tyrode's solution for 5 min, then the displacement traces of the thin pillar from the same sample were recorded.

2.13. Displacement measurement and force calculation

Displacement of the thin pillar was measured under an optical microscope using a 20× objective lens with its focus at the height of the tissue. Customized software that can track the pillar edge and record the trace was developed in-house. Pillar displacement traces were exported and analyzed using customized MATLAB scripts. Displacement (w) of the thin pillar for each sample was found using the scripts and averaged.

We assumed that the thin bendable pillar can be modeled as a rectangular cantilever beam with a fixed end and a free end, experiencing a concentrated force (F) at a given point along the cantilever. The cantilever displacement (w) as a function of height from the fixed end (x) is related to corresponding total force (F) produced by the tissue by Eqs. (1) and (2), derived from Euler–Bernoulli beam theory [24–26]. The other terms in the equation include pillar geometry in term of second moment of inertia (I), modulus (E), and tissue height (a) from the fixed end. After rearranging the quation, the force (F) produced by the tissue to bend the pillar by a displacement (w) was calculated using Eq. (3). Force per unit tissue area was calculated based on tissue dimension shown in Supplementary Fig. 4, assuming a rectangular tissue cross-sectional area.

$$w(x) = \frac{Fx^2}{6EI}(3a - x) \quad \text{for } 0 < x < a \tag{1}$$

$$w(x) = \frac{Fx^2}{6EI}(3x - a) \quad \text{for } 0 < a < x \tag{2}$$

$$F = \frac{6EIw}{2a^3} \quad \text{when } x = a \tag{3}$$

2.14. Image acquisition and processing

Brightfield and fluorescence images of the samples were acquired using a Leica DMI 6000B microscope (Leica Microsystems) using a 5× objectives. Confocal microscope images were acquired with a 40×, 0.8NA water-immersion objective attached to an Olympus FV1000 microscope (Olympus America, Inc.). ImageJ (National Institutes of Health) was used to merge channels, generate z-projection and carry out measurements for images and stacks.

2.15. Quantification of the sarcomere length and orientation

Both sarcomere length and orientation were measured based on the confocal images of tissues with stained alpha-actinin. Sarcomere length was measured using the line measuring tool and profile tool in ImageJ. An intensity profile along 4–6 sarcomere band was generated from each line measurement and an average sarcomere length was calculated from the distance of adjacent bands. Sarcomere orientation was analyzed using the directionality tool in ImageJ. A directionality profile was generated from each measurement.

2.16. Statistical analysis

Sample populations with 3 or more conditions were compared using one-way ANOVA with Tukey's post hoc test to compare multiple conditions. For paired comparison of treated and untreated samples, two-tailed paired t-test was performed. P value smaller than 0.05 was used as the threshold for statistical significance. Data points on the graphs represent mean values with error bars representing standard error of mean (SEM). All statistical analysis was carried out using GraphPad Prism version 6.0 (GraphPad Software).

3. Results

3.1. 3D printing of the micro-pillar platform as a force gauge

To build the micro-pillar platform in a high throughput fashion, we used μCOP to print an array of micro-pillars on a coverslip that can be placed into the well of regular 24-well and 96-well plate (Fig. 1). The customized μCOP 3D printing system consists of a light source, a DMD chip loaded with user-defined pattern, projection optics and a movable printing stage (Fig. 1A). A digital printing pattern consisting of an array of 8 sets of micro-pillars surrounded by their corresponding borders was initially designed and uploaded to a computer prior printing (Fig. 1A and B). Selective parts of the digital pattern can be turned on and off in a user defined fashion throughout the printing process to refine printed structure. As shown in Fig. 1C and D, the array of 8 micro-pillar sets within their

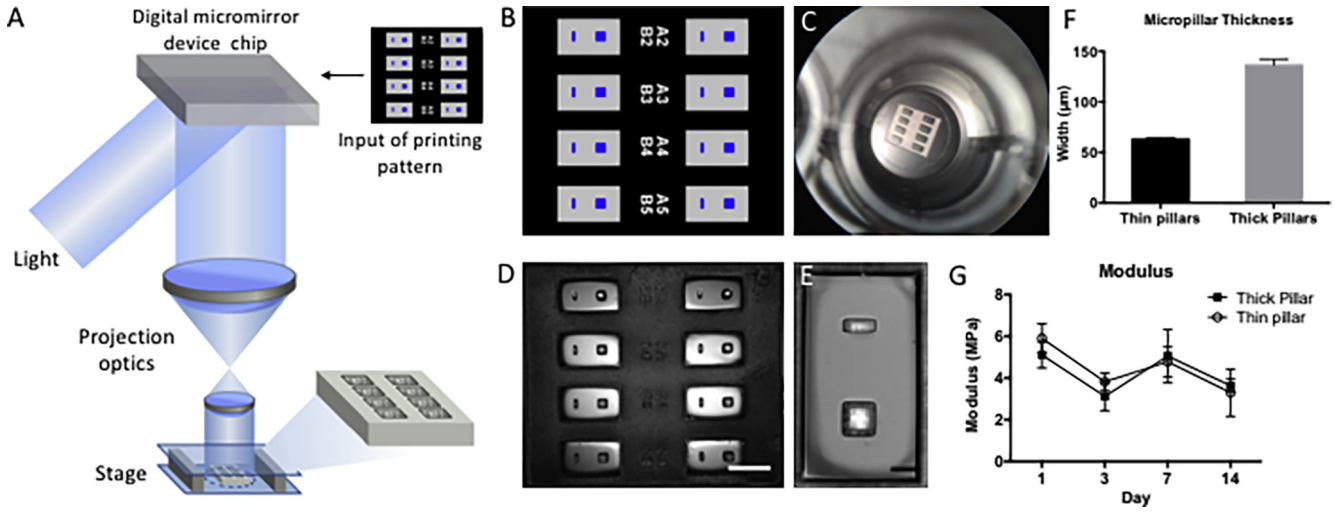

Fig. 1. 3D printing of micro-pillar platform as force gauge. (A) Schematic diagram showing 3D printing platform with customized pattern input and printed construct. (B) Design of digital pattern for printing the force gauge array. (C) Image showing the printed construct fitting into a 96-well plate well. (D) Image of printed construct, scale bar = 500 μm. (E) Magnified image of a single pair of pillars in a micro-well, scale bar = 100 μm. (F) Bar chart showing dimension of the two pillars. n = 6. (G) Plot showing the moduli of pillars over time, n = 5. Error bars represent SEM for all data points.

corresponding micro-wells were fabricated simultaneously within 30 s. The micro-pillar set was designed as a force gauge for cardiac force measurement with two pillars of different sizes: the thick one acting as an anchor and the thin one serving as a bendable cantilever (Fig. 1E). The dimensions of the pillars was consistent throughout prints with the thin pillar measuring 60 × 135 μm and the thick pillar measuring 135 × 135 μm wide (Fig. 1F). The entire construct was 500 μm tall. To better understand the mechanical properties of the pillar in an environment compatible with cell culture conditions, we characterized the moduli of the micro-pillars over 7 days of incubation in cell culture medium at 37 °C. Both the thin and thick pillars yielded a modulus of approximately 4 MPa over 14 days, confirming that the material property remained relatively stable regardless of printed geometry and time during *in-vitro* culture carried out in PBS at 37 °C and 5% CO_2 (Fig. 1G).

3.2. Characterization of human iPSC-derived cardiac tissue on the force gauge

Human iPSC-CMs were mixed with collagen-based gel and centrifuged into the micro-wells of each 3D printed construct. Over 7 days, cardiomyocytes inside the wells elongated and formed a band of cardiac tissue wrapping around the two micro-pillars (Fig. 2A). Deflection of the thin pillar can be observed as early as day 3 following seeding and after 7 days of culture (Supplementary Video 1). Immunofluorescence staining was performed to visualize the sarcomeres and the confocal images were analyzed (Fig. 2B). To maximize the force production, sarcomere alignment of cardiomyocytes in the micro-tissue was promoted to be in the direction of contractile force. This was achieved by varying the inter-pillar distance. As a significant advantage of the rapid 3D printing system, the force gauge constructs with various inter-pillar distances, 175, 200, and 225 μm, were printed, and tested first with neonatal mouse ventricular cardiomyocytes (NVCM) (Supplementary Fig. 1). NVCMs, as a less expensive cell source, were used in this design optimization stage. Sarcomere alignment of the NVCMs were compared among the 3 conditions and a maximal amount of CMs with sarcomeres aligning with the pillar bending direction was found at an inter-pillar distance of 225 μm (Supplementary Fig. 1). From these results, an inter-pillar distance of 225 μm was then used for human iPSC-CM and all later studies. The sarcomere angle distribution of iPSC-CMs was consistent to that of the NVCMs at 225 μm inter-pillar distance (Fig. 2C). Specifically, around 31.7% of cells have their sarcomeres lie within ±15° to the force direction. There were additional 16.9% cells lie at ±30° to the force direction, 14.8% at ±45°, 13.2% at ±60°, 12.9% at ±75°, and 10.5% cells at right angle to the force direction. In addition, an average sarcomere length of 1.8 (±0.06) μm was found in the human iPSC-CMs on pillar, consistent with the working range of human cardiac sarcomeres [27].

3.3. 3D culture on the force gauge with pacing supports cardiac maturation

With good remodeling around the force gauge and optimized sarcomere alignment, steps to further improve human iPSC-CM maturation and produce a higher force were explored. 3D aligned culture, electrical pacing, and mechanical stretching were all reported to enhance stem cell derived-CM maturation during *in-vitro* culture [8–12]. Electrical pacing following 3 days on pillar and mechanical stretching of iPSC-CM before seeding into micro-wells were applied respectively. We compared the 4 different combinations of these approaches using our aligned 3D culture on the force gauge and analyzed their gene expression (Fig. 3A). 3D aligned culture on pillar, as shown as the second approach in Fig. 3, enhanced the overall expression of mature cardiac genes including TNNT, MYH7, MYH6, MLC2C, DES, CNX43, and RYR2 when compared to the 2D culture alone (Fig. 3B). The 3D culture on pillars with additional electrical pacing, as shown as the third approach, significantly improved the expression of genes involved in sarcomere force generation (TNNT, MYH7, MYH6, MLC2C, DES), gap junction (CNX43), and calcium ion channel (RYR2 and CACNA1C) as compared to the 2D approach (Fig. 3B). When compared to the second approach, the additional pacing promoted the overall expression of genes involved in gap junction (CNX43) and calcium ion handling (RYR2 and CACNA1C) (Fig. 3B). The use of mechanically stretched cardiomyocytes before seeding on the force gauge, however, did not provide significant enhancement of gene expression when compared to the condition (third approach) where non-stretched cells were used.

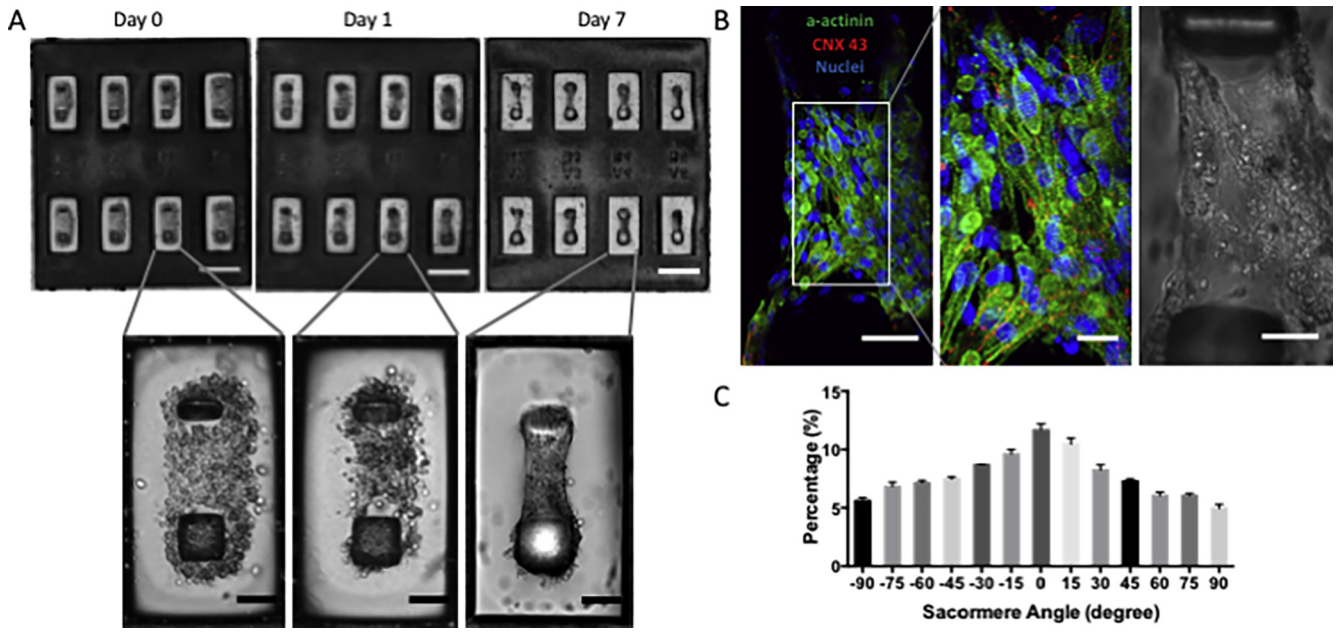

Fig. 2. Characterization of human iPSC-derived cardiac tissue on force gauge. (A) Bright field images showing remodeling of iPSC-CMs following seeding into the micro-wells over time, scale bar = 500 μm (white) and 100 μm (black), respectively. (B) Immunofluorescence image (left), enlarged Immunofluorescence image (middle) magnifying sarcomere structure, and corresponding bright field image (right) showing tissues stained with alpha-actinin (green), connexin 43 (Red), and nuclei (blue). Scale bar = 50 μm (left and right) and 20 μm (middle), respectively. (C) Plot showing the percentage distribution of sarcomere angles from −90° to +90° respective to pillar bending direction, $p < 0.0001$ for one way ANOVA test, and the percent population in 0° to the force direction is significantly higher than those in all other groups except for the +15° group from Tukey's post-hoc test. Error bars represent SEM, n = 3 for all data points. (For interpretation of the references to color in this figure legend, the reader is referred to the web version of this article.)

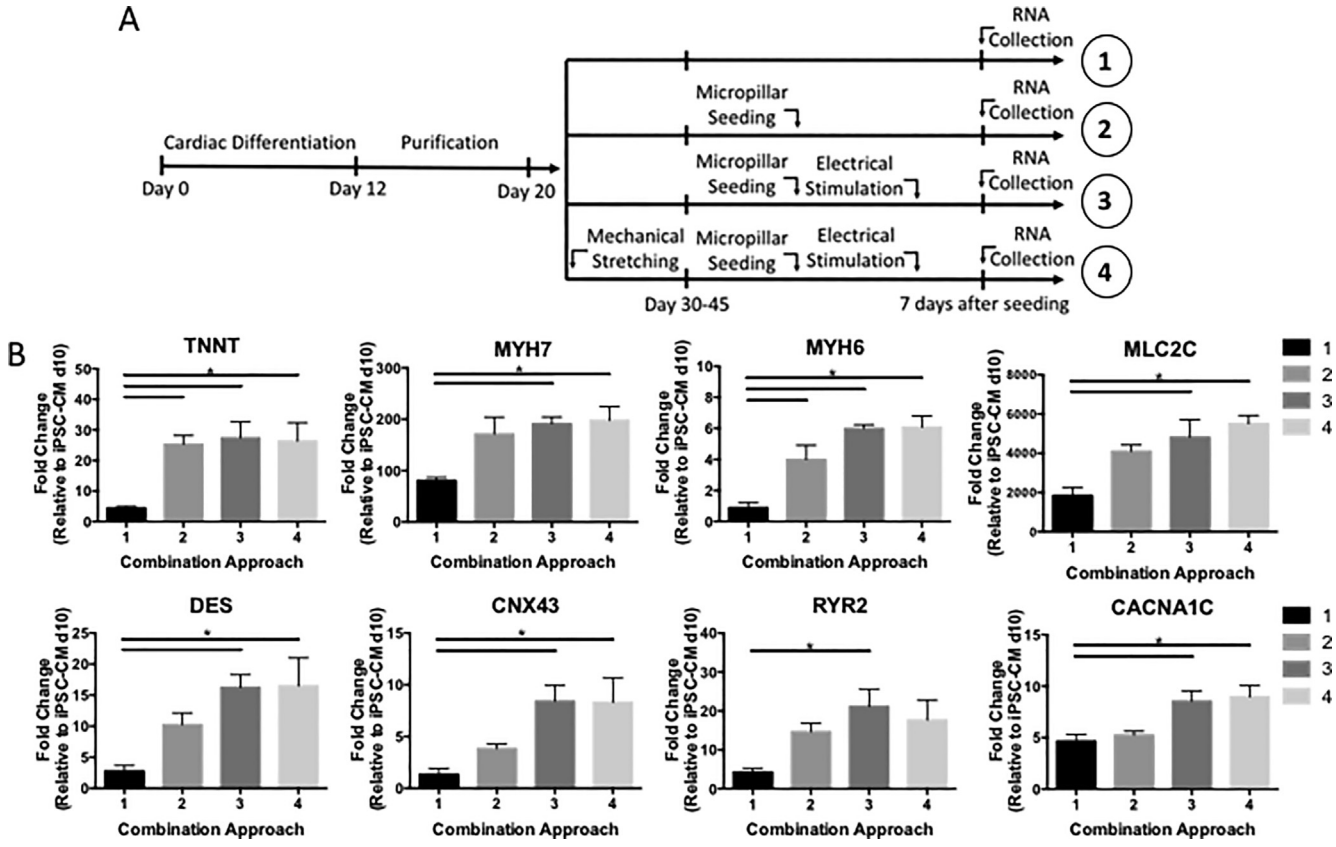

Fig. 3. 3D micro-pillar with electrical pacing supports cardiac maturation. (A) Schematic diagram outlining the 4 maturation approaches for comparison. (B) Plots showing the gene expression fold change of iPSC-CM cultured using various approaches for *TNNT, MYH7, MYH6, MLC2C, DES, CNX43, RYR2* and *CACNA1C*. Error bars represent SEM, n = 3–4, $^*P \leq 0.05$.

3.4. Force measurement and drug response of the human cardiac tissue

Following optimization on the method used to promote tissue maturation, we proceeded to evaluate their force generation based on the observed displacement. The thin pillar displacement was tracked and recorded under a 20X objective lens (Supplementary Video 2 and Supplementary Fig. 5). Force generation was calculated based on the average displacement, thin pillar mechanical property and geometry. An average force of around 8.4 μN was produced by the human iPSC-derived cardiac tissues on day 7 when paced at 0.3 Hz. When normalized to the tissue area, the average unit forces are 1.7 mN/mm^2. We then tested the tissue responses on day 7 with 3 different drugs: ISO (100 nM), LEVO (1 μM), and OM (200 nM). The displacement traces of the thin pillar due to cardiac tissue contraction were recorded before (paired untreated control) and after treating the micro-tissue with the specific drug (Supplementary Fig. 2). Significantly increased pillar displacements by the cardiac micro-tissue were observed following the treatments of ISO, LEVO, and OM (Fig. 4A). Forces generated by the tissue were calculated from the thin pillar modulus on day 7 (Fig. 4B and C). Greater forces were generated by the cardiac micro-tissue following the treatments of all 3 drugs (Fig. 4B). Compared to untreated controls, the cardiac tissue showed an average of 52.0% increase in force after ISO treatment, 36.7% increase after LEVO treatment, and over 63.0% increase after OM treatment (Fig. 4D).

4. Discussion

Traditional ways of studying cardiac tissue contraction and force generation range from single cell studies based on patch clamp to cardiac tissue wire platforms [28,29]. The study of single cardiomyocyte provides insightful understanding on the cellular force generation but is very limited in translating the results to the performance of an aligned cardiac tissue. While a tissue wire platform can provide some information on tissue-level cardiac functional output, the platform design of the tissue wire as well as many other recent human cardiac tissue chips makes it hard to fit into high-throughput screening applications. Without the potential to increase both tissue maturation and force measurement, the use of iPSC-CM tissue in translatable drug screening is still limited. To address these limitations, the goal of this study was to develop a rapid 3D printed force gauge platform that enables the formation of a multicellular cardiac tissue and can be placed into 24-well or 96-well plates to enable in-culture iPSC-derived cardiac tissue maturation and force measurement.

In this work, the use of μCOP technology enabled flexible design of pillar arrays as well as rapid and precise fabrication of micro-scale force gauges. The use of digital pattern design offered great flexibility to fabricate and modify customized 3D structures, thus demonstrating a significant advantage during design optimization compared to conventional molding methods using PDMS [20,30–33]. The constructs were printed on coverslip of various sizes that can fit into a single well of either a 24-well or 96-well plate and at same time facilitated potential analysis handling without directly touching the structure. The micro-scale force gauge was made of one thin pillar as the bendable cantilever and one thick pillar as the anchor for the cardiac tissue. This design simplified the data acquisition and analysis process by focusing only on the thin pillar displacement and using simple beam deflection model for force calculation. Past studies on cardiac force measurement platform all implemented two symmetrical pillar design [13,34]. The need of recording displacement from both pillar complicates the force calculation and analysis process. The mechanical property of both pillars remained consistent over 14 days, which covered the entire 7 day experimental process. This demonstrated the robustness of the materials and 3D printing method. Nevertheless, the average modulus of the thin pillar seeded with cells (Fig. 4C) was slightly lower than that without cells (Fig. 1G), suggesting that the seeding and culture process with cells potentially weaken the thin pillar. The final force calculation was based on the moduli obtained from samples seeded with cells to ensure accurate calculation.

Following the incorporation of iPSC-CMs to the 3D printed pillar array, cardiac tissue bands were formed around the two pillars consistently over 7 days. Having an array of 8 tissues in the same well not only made optimal use of valuable cells but also provided

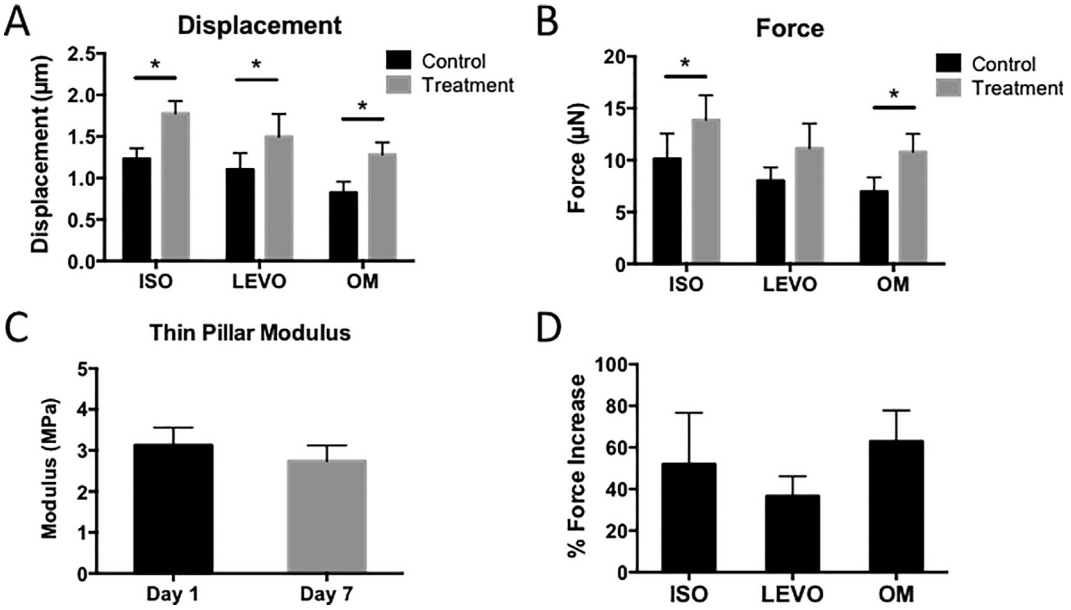

Fig. 4. Human micro-cardiac tissue force measurement and drug response. (A) Bar chart showing the displacement of thin pillar over time before and after treating ISO, LEVO or OM paced at 0.3 Hz. (B) Bar chart showing force generated before and after treating ISO, LEVO or OM when paced at 0.3 Hz. (C) Bar chart showing the mechanical property of thin pillar with iPSC-CM seeded on day 1 and 7. (D) Bar chart showing the percentage force increase after treatment with ISO, LEVO or OM at 0.3 Hz pacing. Error bars represent SEM, and n = 5 for all data points, *P ≤ 0.05.

multiple repeats for each experimental condition. This array design provided the potential to study more drug candidates in a single plate. Such throughput was not achieved by current EHT systems [10,13]. Following 7 days, cardiac tissue on pillar exhibited visible displacement of the thin pillar with largely aligned sarcomeres. Within the same well size, best sarcomere alignment was achieved with an inter-pillar distance of 225 μm, indicating that this design has the highest potential for large force generation compared to shorter designs. Potentially better alignment can be achieved by further lengthening the inter-pillar distance, which however will likely require lengthening of the micro-well and thus change the total amount of cells falling into each micro-well and forming the tissue bands. By using this current design, an average cellular sarcomere length of 1.8 μm indicates that a sarcomere length in the working range as in native heart is achieved [27].

Following the consistent establishment of physiologically relevant human cardiac tissues, we aimed to improve iPSC-derived tissue maturation. 3D aligned culture, mechanical stretching and electrical pacing, as proven methods to promote cardiomyocyte maturation, had been adopted in various combinations to find the optimal approach [8–12]. The upregulation of key genes involved in force generation, electrical signal propagation, and calcium signaling by 3D aligned culture on pillars when compared to 2D culture was confirmed with literature findings [8,9,35]. The addition of in-culture pacing further promoted the significant upregulation of genes related calcium channel, which is consistent with past reports [36]. However, mechanical stretching of iPSC-CMs prior to their digestion for tissue band formation on the pillar had no significant improvements on any of the gene expressions. Therefore, we conclude that among the 4 approaches tested, the 3D aligned culture on pillar with in-culture pacing is sufficient and no prior mechanical stretching before seeding is necessary. Nevertheless, the stretching frequency in this study was performed on the lower end of the range used in literature [37–39], i.e. 0.5 Hz to match the spontaneous beating rate of the cells. Using higher frequencies could potentially induce more maturation. In addition, future studies on using human primary adult cardiomyocytes would be a valuable reference to further enhance the understanding on tissue maturation level.

After promoting tissue maturation by 3D aligned culture with in-culture pacing, we carried out force measurements directly using an optical microscope. In particular, we compared the force production level across various types of platforms including both the single cell setup and other micro-scale EHT or millimeter long tissue wire setup. For the studies on force produced by single human iPSC-derived cardiomyocyte, force in the range of 0.01–0.2 μN was reported [40,41]. The force from a single cell is much lower and is not comparable to the tissue level contractile force reported by any of the current platforms. When comparing with other microscopic EHT setup using tissue that was around 3 times longer and twice the width of our tissue, a force in the similar range, i.e. 5–15 μN was reported [34]. Therefore, the unit force normalized by tissue's cross-sectional area produced by our tissue is higher. When comparing with millimeter long cardiac tissue wire, the overall force produced by the tissue wire platform was reported to be around 100–150 μN, 10 times the total force produced from a micro-scale tissue [10,13]. However, when looking at a unit force normalized by the tissue's cross-sectional area, tissue wire reported up to 1.2 mN/mm^2 [10], still lower than the average unit force of 1.7 mN/mm^2 reported in our study using the micro-scale tissue. The comparison with other existing platforms, in particular with current micro-scale platforms and tissue wire platforms, shows that our system produces a higher force and can work with a high throughput well plate setup. The force difference can be caused by the matrix and cantilever stiffness used, based on study showing higher force produced from a stiffer matrix and cantilever used [34]. Other potential causes can be the difference in maturation level of cells as well as the maturation approach used for stem cell derived cardiac tissues. In addition, we observed a force increase following treatment of ISO, beta adrenergic agonist, LEVO, a calcium sensitizer, and OM, a cardiac myosin activator. In particular, the demonstrated increase in contractile force by our human cardiac tissue when treated with LEVO and OM is consistent with past findings using isolated muscle samples and animal models [42–45]. No prior studies using engineered human cardiac tissues have demonstrated such force increase. Furthermore, with the capability to efficiently measure force generation from cardiac tissue, this engineered platform provides possibility for future work on studying how the differences in degree of cell alignment, maturation gene expression, and culture conditions are related to variation in force production.

Various platforms have been developed over the past decade to promote the maturation of human iPSC-derived cardiac tissues and evaluate their performance. Nevertheless, few achievements have been made to combine tissue maturation scheme with a force gauge platform while at the same time miniaturizing the design to fit into high throughput well plate setup. By demonstrating large force generation and consistent drug response with animal studies, our 3D printed micro-scale force gauge array serves as a promising platform in promoting mature cardiac gene expression in human iPSC-CMs, measuring force generation, and studying drug responses in a high-throughput fashion. With its high throughput fabrication potential and great design flexibility, 3D printing serves as a promising tool to build miniaturized cardiac tissues for high-throughput in-vitro drug screening applications. Future studies that incorporate patient-specific cells, thorough biological and functional characterizations, automated handling and data acquisition system could transform this prototypic system to patient-specific high throughput screening platforms.

Acknowledgements

The authors would like to thank Dr. Farah Sheikh and Dr. Fabian Zanella for providing in-house reprogrammed human iPSCs and supporting iPSC culture and differentiation. This project is supported in part by grants from the California Institute for Regenerative Medicine (Grant no. RT3-07899), National Institutes of Health (Grant # EB021857 and HL137100) and National Science Foundation (Grant 1644967). The authors also would like to acknowledge the University of California San Diego Neuroscience Microscopy Shared Facility funded through NS047101. Scholarship funding for Dr. Claire Yu was provided by the Natural Sciences and Engineering Research Council (NSERC) Postdoctoral Fellowship Scholarship of Canada.

ADM is a co-founder of and has an equity interest in Insilicomed, Inc., and he serves on the scientific advisory board. Some of his research grants, including those acknowledged here, have been identified for conflict of interest management based on the overall scope of the project and its potential benefit to Insilicomed, Inc. The author is required to disclose this relationship in publications acknowledging the grant support, however the research subject and findings reported here did not involve the company in any way and have no relationship with the business activities or scientific interests of the company. The terms of this arrangement have been reviewed and approved by the University of California San Diego in accordance with its conflict of interest policies. The other authors have no competing interests to declare.

Appendix A. Supplementary data

Supplementary data to this article can be found online at https://doi.org/10.1016/j.actbio.2018.12.026.

References

[1] S. Sidney, C.P. Quesenberry, M.G. Jaffe, M. Sorel, M.N. Nguyen-Huynh, L.H. Kushi, A.S. Go, J.S. Rana, Recent trends in cardiovascular mortality in the United States and public health goals, JAMA Cardiol. 1 (2016) 594, https://doi.org/10.1001/jamacardio.2016.1326.

[2] A. Prashant, Global challenges in cardiovascular drug discovery and clinical trials, Mol. Biol. 06 (2017) 1–4, https://doi.org/10.4172/2168-9547.1000193.

[3] G. Gromo, J. Mann, J.D. Fitzgerald, Cardiovascular drug discovery: a perspective from a research-based pharmaceutical company, Cold Spring Harb. Perspect. Med. 4 (2014), https://doi.org/10.1101/cshperspect.a014092.

[4] J.C. del Álamo, D. Lemons, R. Serrano, A. Savchenko, F. Cerignoli, R. Bodmer, M. Mercola, High throughput physiological screening of iPSC-derived cardiomyocytes for drug development, Biochim. Biophys. Acta – Mol. Cell Res. 2016 (1863) 1717–1727, https://doi.org/10.1016/J.BBAMCR.2016.03.003.

[5] A.S.T. Smith, J. Macadangdang, W. Leung, M.A. Laflamme, D.-H. Kim, Human iPSC-derived cardiomyocytes and tissue engineering strategies for disease modeling and drug screening, Biotechnol. Adv. 35 (2017) 77–94, https://doi.org/10.1016/J.BIOTECHADV.2016.12.002.

[6] J.T. Koivumäki, N. Naumenko, T. Tuomainen, J. Takalo, M. Oksanen, K.A. Puttonen, Š. Lehtonen, J. Kuusisto, M. Laakso, J. Koistinaho, P. Tavi, Structural immaturity of human iPSC-derived cardiomyocytes: In silico investigation of effects on function and disease modeling, Front. Physiol. 9 (2018) 80, https://doi.org/10.3389/fphys.2018.00080.

[7] S. Casini, A.O. Verkerk, C.A. Remme, Human iPSC-derived cardiomyocytes for investigation of disease mechanisms and therapeutic strategies in inherited arrhythmia syndromes: strengths and limitations, Cardiovasc. Drugs Ther. 31 (2017) 325–344, https://doi.org/10.1007/s10557-017-6735-0.

[8] T. Nakane, H. Masumoto, J.P. Tinney, F. Yuan, W.J. Kowalski, F. Ye, A.J. LeBlanc, R. Sakata, J.K. Yamashita, B.B. Keller, Impact of cell composition and geometry on human induced pluripotent stem cells-derived engineered cardiac tissue, Sci. Rep. 7 (2017) 45641, https://doi.org/10.1038/srep45641.

[9] G.J. Scuderi, J. Butcher, Naturally engineered maturation of cardiomyocytes, Front. Cell Dev. Biol. 5 (2017) 50, https://doi.org/10.3389/fcell.2017.00050.

[10] W. Zhang, C.W. Kong, M.H. Tong, W.H. Chooi, N. Huang, R.A. Li, B.P. Chan, Maturation of human embryonic stem cell-derived cardiomyocytes (hESC-CMs) in 3D collagen matrix: effects of niche cell supplementation and mechanical stimulation, Acta Biomater. 49 (2017) 204–217, https://doi.org/10.1016/j.actbio.2016.11.058.

[11] J.-L. Ruan, N.L. Tulloch, M.V. Razumova, M. Saiget, V. Muskheli, L. Pabon, H. Reinecke, M. Regnier, C.E. Murry, Mechanical stress conditioning and electrical stimulation promote contractility and force maturation of induced pluripotent stem cell-derived human cardiac tissue, Circulation 134 (2016) 1557–1567, https://doi.org/10.1161/CIRCULATIONAHA.114.014998.

[12] Y.-C. Chan, S. Ting, Y.-K. Lee, K.-M. Ng, J. Zhang, Z. Chen, C.-W. Siu, S.K.W. Oh, H.-F. Tse, Electrical stimulation promotes maturation of cardiomyocytes derived from human embryonic stem cells, J. Cardiovasc. Transl. Res. 6 (2013) 989–999, https://doi.org/10.1007/s12265-013-9510-z.

[13] I. Mannhardt, K. Breckwoldt, D. Letuffe-Brenière, S. Schaaf, H. Schulz, C. Neuber, A. Benzin, T. Werner, A. Eder, T. Schulze, B. Klampe, T. Christ, M.N. Hirt, N. Huebner, A. Moretti, T. Eschenhagen, A. Hansen, Human engineered heart tissue: analysis of contractile force, Stem Cell Rep. 7 (2016) 29–42, https://doi.org/10.1016/j.stemcr.2016.04.011.

[14] E. D'Arcangelo, A.P. McGuigan, Micropatterning strategies to engineer controlled cell and tissue architecture in vitro, Biotechniques 58 (2015), https://doi.org/10.2144/000114245.

[15] D. Kim, P.T.C. So, High-throughput three-dimensional lithographic microfabrication, Opt. Lett. 35 (2010) 1602–1604, https://doi.org/10.1364/OL.35.001602.

[16] K.C. Hribar, D. Finlay, X. Ma, X. Qu, M.G. Ondeck, P.H. Chung, F. Zanella, A.J. Engler, F. Sheikh, K. Vuori, S. Chen, Nonlinear 3D projection printing of concave hydrogel microstructures for long-term multicellular spheroid and embryoid body culture, Lab Chip. 15 (2015) 2412–2418, https://doi.org/10.1039/C5LC00159E.

[17] X. Ma, X. Qu, W. Zhu, Y.-S. Li, S. Yuan, H. Zhang, J. Liu, P. Wang, C.S.E. Lai, F. Zanella, G.-S. Feng, F. Sheikh, S. Chien, S. Chen, Deterministically patterned biomimetic human iPSC-derived hepatic model via rapid 3D bioprinting, Proc. Natl. Acad. Sci. U.S.A. 113 (2016) 2206–2211, https://doi.org/10.1073/pnas.1524510113.

[18] W. Zhu, X. Ma, M. Gou, D. Mei, K. Zhang, S. Chen, 3D printing of functional biomaterials for tissue engineering, Curr. Opin. Biotechnol. 40 (2016) 103–112, https://doi.org/10.1016/j.copbio.2016.03.014.

[19] W. Zhu, X. Qu, J. Zhu, X. Ma, S. Patel, J. Liu, P. Wang, C.S.E. Lai, M. Gou, Y. Xu, K. Zhang, S. Chen, Direct 3D bioprinting of prevascularized tissue constructs with complex microarchitecture, Biomaterials 124 (2017) 106–115, https://doi.org/10.1016/j.biomaterials.2017.01.042.

[20] P. Soman, P.H. Chung, A.P. Zhang, S. Chen, Digital microfabrication of user-defined 3D microstructures in cell-laden hydrogels, Biotechnol. Bioeng. 110 (2013) 3038–3047, https://doi.org/10.1002/bit.24957.

[21] S. Tohyama, F. Hattori, M. Sano, T. Hishiki, Y. Nagahata, T. Matsuura, H. Hashimoto, T. Suzuki, H. Yamashita, Y. Satoh, T. Egashira, T. Seki, N. Muraoka, H. Yamakawa, Y. Ohgino, T. Tanaka, M. Yoichi, S. Yuasa, M. Murata, M. Suematsu, K. Fukuda, Distinct metabolic flow enables large-scale purification of mouse and human pluripotent stem cell-derived cardiomyocytes, Cell Stem Cell 12 (2013) 127–137, https://doi.org/10.1016/j.stem.2012.09.013.

[22] A. Ludke, G. Akolkar, P. Ayyappan, A.K. Sharma, P.K. Singal, Time course of changes in oxidative stress and stress-induced proteins in cardiomyocytes exposed to doxorubicin and prevention by vitamin C, PLoS One. 12 (2017), https://doi.org/10.1371/journal.pone.0179452 e0179452.

[23] H. Kim, S. Bae, Y. Kim, C.-H. Cho, S.J. Kim, Y.-J. Kim, S.-P. Lee, H.-R. Kim, Y. Hwang, J.S. Kang, W.J. Lee, Vitamin C prevents stress-induced damage on the heart caused by the death of cardiomyocytes, through down-regulation of the excessive production of catecholamine, TNF-α, and ROS production in Gulo(−/−) mice, Free Radic. Biol. Med. 65 (2013) 573–583, https://doi.org/10.1016/j.freeradbiomed.2013.07.023.

[24] W. Flügge, Handbook of engineering mechanics, 1st ed., McGraw-Hill, 1962. doi:10.1115/1.3630093.

[25] O.A. Bauchau, J.I. Craig, Euler-Bernoulli beam theory, in: Struct. Anal., Springer, Dordrecht, 2009, pp. 173–221, https://doi.org/10.1007/978-90-481-2516-6_5.

[26] J.W. Gardner, V.K. Varadan, O.O. Awadelkarim, Microsensors, MEMS, and SMART Devices, John Wiley & Sons Ltd, 2013. doi: 10.1002/9780470846087.

[27] L.M. Hanft, F.S. Korte, K.S. McDonald, Cardiac function and modulation of sarcomeric function by length, Cardiovasc. Res. 77 (2008) 627–636, https://doi.org/10.1093/cvr/cvm099.

[28] V.Y. Sidorov, P.C. Samson, T.N. Sidorova, J.M. Davidson, C.C. Lim, J.P. Wikswo, I-Wire Heart-on-a-Chip I: three-dimensional cardiac tissue constructs for physiology and pharmacology, Acta Biomater. 48 (2017) 68–78, https://doi.org/10.1016/j.actbio.2016.11.009.

[29] E.S. Richardson, Y.-F. Xiao, Electrophysiology of Single Cardiomyocytes: patch Clamp and Other Recording Methods, in: Card. Electrophysiol. Methods Model, Springer, US, Boston, MA, 2010, pp. 329–348, https://doi.org/10.1007/978-1-4419-6658-2_16.

[30] X. Qu, W. Zhu, S. Huang, Y. Li, S. Chien, K. Zhang, Relative impact of uniaxial alignment vs form-induced stress on differentiation of human adipose derived stem cells, Biomaterials 34 (2013) 9812–9818.

[31] T.Q. Huang, X. Qu, J. Liu, S. Chen, 3D printing of biomimetic microstructures for cancer cell migration, Biomed. Microdevices 16 (2014) 127–132, https://doi.org/10.1007/s10544-013-9812-6.

[32] M. Gou, X. Qu, W. Zhu, M. Xiang, J. Yang, K. Zhang, Y. Wei, S. Chen, Bio-inspired detoxification using 3D-printed hydrogel nanocomposites, Nat. Commun. 5 (2014) 3774, https://doi.org/10.1038/ncomms4774.

[33] W. Zhu, J. Li, Y.J. Leong, I. Rozen, X. Qu, R. Dong, Z. Wu, W. Gao, P.H. Chung, J. Wang, S. Chen, 3D-printed artificial microfish, Adv. Mater. 27 (2015) 4411–4417, https://doi.org/10.1002/adma.201501372.

[34] T. Boudou, D. Ph, W.R. Legant, A. Mu, M.A. Borochin, N. Thavandiran, M. Radisic, P.W. Zandstra, J.A. Epstein, K.B. Margulies, C.S. Chen, A Microfabricated Platform to Measure and Manipulate the Mechanics of Engineered Cardiac Microtissues, 18 (2012) pp. 910–919. doi:10.1089/ten.tea.2011.0341.

[35] R.R. Besser, M. Ishahak, V. Mayo, D. Carbonero, I. Claure, A. Agarwal, Engineered microenvironments for maturation of stem cell derived cardiac myocytes, Theranostics 8 (2018) 124–140, https://doi.org/10.7150/thno.19441.

[36] S. Baumgartner, M. Halbach, B. Krausgrill, M. Maass, S.P. Srinivasan, R.G.A. Sahito, G. Peinkofer, F. Nguemo, J. Müller-Ehmsen, J. Hescheler, Electrophysiological and morphological maturation of murine fetal cardiomyocytes during electrical stimulation in vitro, J. Cardiovasc. Pharmacol. Ther. 20 (2015) 104–112, https://doi.org/10.1177/1074248414536273.

[37] W.L. Stoppel, D.L. Kaplan, L.D. Black, Electrical and mechanical stimulation of cardiac cells and tissue constructs, Adv. Drug Deliv. Rev. 96 (2016) 135–155, https://doi.org/10.1016/j.addr.2015.07.009.

[38] J.G. Jacot, H. Kita-Matsuo, K.A. Wei, H.S. Vincent Chen, J.H. Omens, M. Mercola, A.D. McCulloch, Cardiac myocyte force development during differentiation and maturation, in: Ann. N. Y. Acad. Sci., NIH Public Access, 2010: pp. 121–127. doi:10.1111/j.1749-6632.2009.05091.x.

[39] M.G.V. Petroff, S.H. Kim, S. Pepe, C. Dessy, E. Marbán, J.L. Balligand, S.J. Sollott, Endogenous nitric oxide mechanisms mediate the stretch dependence of Ca2+release in cardiomyocytes, Nat. Cell Biol. 3 (2001) 867–873, https://doi.org/10.1038/ncb1001-867.

[40] A.J.S. Ribeiro, Y.-S. Ang, J.-D. Fu, R.N. Rivas, T.M.A. Mohamed, G.C. Higgs, D. Srivastava, B.L. Pruitt, Contractility of single cardiomyocytes differentiated from pluripotent stem cells depends on physiological shape and substrate stiffness, Proc. Natl. Acad. Sci. U.S.A. 112 (2015) 12705–12710, https://doi.org/10.1073/pnas.1508073112.

[41] M.L. Rodriguez, B.T. Graham, L.M. Pabon, S.J. Han, C.E. Murry, N.J. Sniadecki, Measuring the contractile forces of human induced pluripotent stem cell-derived cardiomyocytes with arrays of microposts, J. Biomech. Eng. 136 (2014), https://doi.org/10.1115/1.4027145 051005.

[42] E. du Toit, D. Hofmann, J. McCarthy, C. Pineda, Effect of levosimendan on myocardial contractility, coronary and peripheral blood flow, and arrhythmias during coronary artery ligation and reperfusion in the in vivo pig model, Heart 86 (2001) 81–87, https://doi.org/10.1136/heart.86.1.81.

[43] S. Sato, M.A.H. Talukder, H. Sugawara, H. Sawada, M. Endoh, Effects of levosimendan on myocardial contractility and Ca2+transients in aequorin-loaded right-ventricular papillary muscles and indo-1-loaded single ventricular cardiomyocytes of the rabbit, J. Mol. Cell. Cardiol. 30 (1998) 1115–1128, https://doi.org/10.1006/jmcc.1998.0677.

[44] M.S. Utter, D.M. Ryba, B.H. Li, B.M. Wolska, R.J. Solaro, Omecamtiv mecarbil, a cardiac myosin activator, increases ca2+ sensitivity in myofilaments with a dilated cardiomyopathy mutant tropomyosin E54K, J. Cardiovasc. Pharmacol. 66 (2015) 347–353, https://doi.org/10.1097/FJC.0000000000000286.

[45] L. Nagy, Á. Kovács, B. Bódi, E.T. Pásztor, G.Á. Fülöp, A. Tóth, I. Édes, Z. Papp, The novel cardiac myosin activator omecamtiv mecarbil increases the calcium sensitivity of force production in isolated cardiomyocytes and skeletal muscle fibres of the rat, Br. J. Pharmacol. 172 (2015) 4506–4518, https://doi.org/10.1111/bph.13235.